



XA05C0018

## LOCAL DEPOSITION PATTERNS OF INHALED RADON PROGENY IN HUMAN BRONCHIAL AIRWAYS

T. Heistracher<sup>1)</sup>, W. Hofmann<sup>1)</sup> and I. Balásházy<sup>1,2)</sup>

<sup>1)</sup> Institute of Physics and Biophysics, University of Salzburg, Hellbrunner Str.34, A-5020 Salzburg, Austria

<sup>2)</sup> KFKI Atomic Energy Research Institute, Health Physics Department, H-1525 Budapest 114, Hungary

### INTRODUCTION

The local distribution of radon decay products deposited within bronchial bifurcations, particularly the formation of hot spots, may be more relevant for the determination of cellular doses in bronchial tissue than the commonly computed deposition efficiency, which is conceptually equivalent to the assumption of a uniform nuclide distribution. It is well known that the initial states of lung cancer in humans preferably occur in upper airways close to the carinal location. In this study we use a recently developed geometric approach of a physiologically realistic bifurcation to demonstrate the site sensitivity of radon progeny deposition for two particle sizes, which are representative of the unattached and attached fraction of radon progeny.

### METHOD

For the calculation of the local deposition sites of radon progeny in bronchial airway bifurcations we apply a three step procedure: First of all, the geometry of the lung bifurcation has to be defined as a numerical mesh. This is done by applying a two-parametric iteration procedure (Heistracher and Hofmann, 1995) to get an unstructured, distorted mesh with about 50.000 node points. Secondly, the air velocity field is computed by applying the computational fluid dynamics (CFD) package FIRE<sup>®</sup> (AVL-List GmbH, Graz, Austria), which uses a finite volume approach to solve the Navier-Stokes and continuity equations for compressible flows (Heistracher and Hofmann, 1993). Thirdly, the inertial and gravitational forces acting on the particles are modeled by the Basset-Boussinesq-Oseen equation (Hofmann and Balásházy, 1991; Balásházy et al., 1991), whereas the effects of Brownian motion are considered by using the Fokker-Plank equation and Maxwell's velocity distribution of the kinetic gas theory. The effect of interception is taken into account by a prismatic intersection technique.

### RESULTS

In Fig. 1 the isoline representation of the velocity field in the main plane (plane of bifurcation) for inspiration ( $60 \text{ l min}^{-1}$  minute volume; left panel) reveals practically no changes in the parabolic character of the flow in the parent branch up to the middle of the central zone (that is the region where the two daughter branches merge), whereas a distinct asymmetry predominates the flow in the daughter branches. Strong secondary motions (which are the velocity components normal to the prevailing flow direction) seem to maintain this situation downstream to the end of the daughter branches.

Parabolic flow dominates the daughter branch regions for expiration ( $60 \text{ l min}^{-1}$ ; right panel of Fig. 1), whereas for the central zone a rather complicated flow situation exists, which leads to the characteristic bulk-shape of the velocity profile across the upstream end of the central zone, extended toward the proximal end of the parent branch.

In this study, we present deposition results for particle sizes of 1 nm (unattached fraction of  $^{222}\text{Rn}$  progeny) and  $0.2 \mu\text{m}$  (attached fraction of  $^{222}\text{Rn}$  progeny).

Fig. 2 shows the deposition patterns for particles with a geometric diameter of 1 nm for inspiration in a narrow bifurcation model, which has a distinct transition from the parent branch to the central zone (left panel), and in a physiologically realistic bifurcation (PRB) model (right panel).

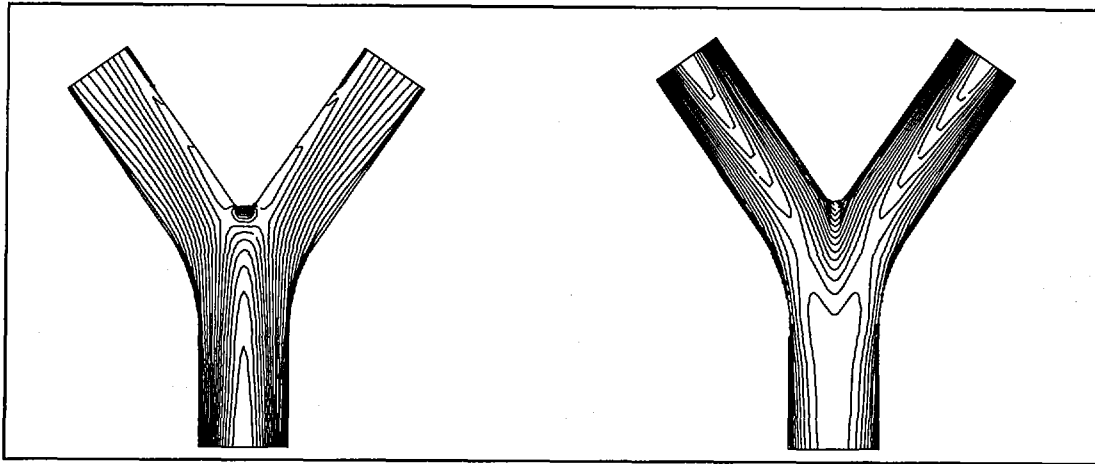


**Fig. 1:** Isoline representation of the velocity field (20 isolines) in the main plane of bifurcation for inspiration (left panel) and expiration (right panel; for parameters used, see Table 1).

As diffusion is the dominant physical process for deposition for this particle size, little enhanced deposition should be found in this case. Due to the very high velocity of inhalation chosen in this study, however, distinct sites of enhanced deposition can be found for inhalation: (i) on the inner sides of the daughter branches close to the carinal ridge, and, (ii) on the upper and lower parts of the central zone. The local minimum of deposition density in the narrow bifurcation model on the outer side of the central zone can be related to the 'dead water zone' immediately after the onset of the central zone.

For exhalation, the sites of enhanced deposition of 1 nm particles are: (iii) upper and lower side of the parent branch, and, (iv) inner and outer side of the daughter branches. The former region has a distinct linear extension in axial direction of the parent branch, whereas the latter is less pronounced.

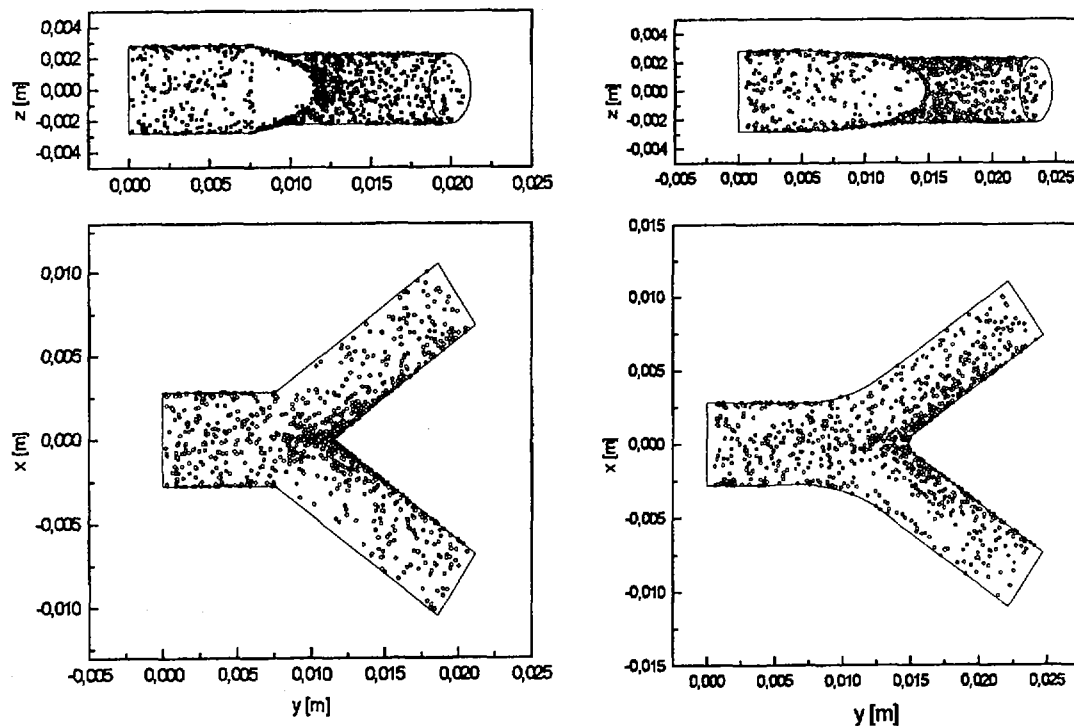


**Fig. 2:** Deposition pattern for 1 nm particles, which are characteristic of the unattached fraction, for inspiration in a narrow bifurcation model (left panel) and for a PRB model (right panel; for parameters used, see Table 1).

For particles with 200 nm geometric diameter the situation is completely different. Due to the well known minimum of the deposition efficiency in this particle size range (Hofmann et al., 1990), a distinct enhancement of deposition cannot be found. The deposition efficiency is reduced by about an order of magnitude compared with the 1 nm particle size. The sites of enhanced deposition for inspiration are on the inner side of the daughter branches close to the carinal ridge and for expiration on the upper and lower side of the parent branch.

## CONCLUSIONS

The local hot spots close to the carina in Fig. 2 emphasize the importance of considering the local distribution of particles deposited in bronchial airway bifurcations. Not only the size of the particles and the breathing conditions, but also the geometric boundary conditions (narrow versus PRB approach) have effect on deposition patterns. Due to the additional fact, that mucociliary clearance is reduced at these sites of enhanced deposition (Hofmann et al., 1990), these findings may have an important impact on risk assessment studies. Further studies have to be conducted to obtain high resolution local deposition density data.

<i>Parameter</i>	<i>Symbol</i>	<i>Unit</i>	<i>Value</i>
Branching angle	$\varphi$	deg	35°
Parent branch length	$L_p$	m	7.6E-3
Parent branch radius	$R_p$	m	2.8E-3
Daughter branch lengths	$L_d$	m	12.7E-3
Daughter branch radii	$R_d$	m	2.25E-3
Carinal ridge curvature*	$c_c$	-	0.1
Branching curvature*	$c_a, c_b$	-	3.0
Averaged inspiratory velocity	$v_{m,i}$	ms <sup>-1</sup>	10.2
Averaged expiratory velocity	$v_{m,e}$	ms <sup>-1</sup>	15.5
Number of particles selected	$n$	-	10.000
Deposition efficiency	$\eta$	-	0.1066
Deposition efficiency*	$\eta$	-	0.0945

**Table 1:** Parameters of bifurcation models used for this study and deposition efficiency results. An asterisk denotes items for the PRB model only.

## ACKNOWLEDGMENTS

This work was funded by the Austrian Fonds zur Förderung der wissenschaftlichen Forschung, Project P10426-ÖME.

## REFERENCES

- Balásházy, I., Hofmann, W., Martonen, T.B. (1991) Inspiratory Particle Deposition in Airway Bifurcation Models. *J. Aerosol. Sci.* 22; No.1, pp 15-30, 1991.
- Heistracher, T., and Hofmann, W. (1995) Physiologically realistic models of bronchial airway bifurcations. *J. Aerosol. Sci.* 26: 497-509.
- Hofmann, W., and Balásházy, I. (1991) Particle Deposition Patterns within Airway Bifurcations - Solution of the 3D Navier-Stokes Equation. *Radiation Protection Dosimetry* Vol. 38, No. 1/3, pp. 57-63.
- Hofmann, W., Martonen, T.B., and Ménache, M. G. (1990) A Dosimetric Model for Localised Radon Progeny Accumulations at Tracheobronchial Bifurcations. *Radiation Protection Dosimetry*, Vol.30, No. 4, pp. 245-259.
- T. Heistracher T., and Hofmann, W. (1993) Airflow in bronchial bifurcations: Development of secondary motions. *J. Aerosol. Sci.*, 24, Suppl. 1, pp. S89-S90.